Scientific Journal Impact Factor (SJIF) : 5.278
International Journal of Modern Trends in Engineering and Research
IJMTER
ISSN (ONLINE) : 2349 - 9745
ISSN (PRINT) : 2393 - 8161

RADIAL BASIS FUNCTION NETWORK BASED HYBRID SOLAR AND BATTERY OPERATED DC-DC CONVERTER SYSTEM

[1]Vinothini S B , [2]G.Dinesh, [3]N.Anandhakumar

[1]M.E, Dept of EEE Mahendra Engineering College
[2,3]Assistant Professor, Dept of EEE Mahendra Engineering College

Abstract: *In this paper, a radial basis function network (RBFN) controller based three-level boost converter is presented for DC/DC conversion in the solar PV (Photovoltaic) –Battery hybrid system. A neural network based RBFN controller is involved in converter control and maximum power point tracking (MPPT) to trace the maximum power point. The three-level boost converters have a wide range of application in power conversion systems with continuous supply current and high voltage gain. Three-level converter configuration can minimize the voltage stress across the switches and also have a capability of maximum energy transfer from input to output through the series connected boost inductors. The maximum efficiency of 91.9% is achieved for the proposed system configuration at 1000W/m2 irradiation and full load. This kind of converter topology is widely used in DC/DC conversion to step up the voltage to the required level based on the application. The boost type converter is essential in low power generating systems such as solar PV systems, fuel cells, switched mode power supply and other DC supplied systems. The suggested three-level converter configuration is an adequate system for solar PV systems.*

Keywords: radial basis function network, Photovoltaic, maximum power point tracking ,PV systems

I. INTRODUCTION

Electricity demand is increasing from the past decades due to excessive utilization of power in various sectors. It becomes very expensive to end users as per economic point view due to high production cost with conventional energy resources such as fossil fuels. In order to overcome the difficulties in power generation to meet the load demand, the government policies and industrial sectors are forced to concentrate towards green energy solutions called Renewable Energy Resources [1, 2]. The renewable energy resources are playing a vital in the power sector due to abundant energy availability in nature such as solar, wind, fuel cell, tidal, thermal and ocean etc. Apart from all, the solar and wind energy conversion systems are the dominant energy resources for eco-friendly energy conversion. Due to immense advancement in low cost and highly efficient power converters, the conversion of renewable energy becomes simple. The installation of solar PV systems [3-4] is quite easy than other form of energy structures. There are many MPPT control techniques [5-6] proposed by the researchers to extract the maximum power from the renewable energy systems such as incremental conductance (INC), Perturbation & Observation (P & O), hill climb method, fuzzy logic [7, 8] and artificial intelligence based

controllers etc. The perturbation & observation and hill climb methods are regularly used MPPT techniques [9-11] in solar and wind energy conversion systems due to simple structures but limited by low power tracking capability and also have low accuracy. This kind of MPPT controllers is essential for solar, wind and fuel cell energy system to trace the maximum power point and also control the DC to DC converters. However, the convergence of the aforementioned MPPT techniques is low and not suitable for non linear systems. Here the PBFN MPPT controller [12] can defeat the drawbacks of conventional MPPT techniques even for non linear systems with fast convergence. The two-level DC to DC boost converters [13-15] plays a significant role in the renewable integration of solar PV and fuel cell energy systems to enhance the voltage level. Due to low efficiency, low power density and high voltage stress across the switches, this kind of converters are replaced by the three-level boost converters [16] which offers high power density and reduced switching losses. The three-level boost converters are widely used in the solar PV systems for DC/DC conversion with low voltage stress across the switches, low ripple content and high efficiency [17]. In this paper, RBFN MPPT controller based three-level boost converter configuration is designed for solar PV system with battery back-up. The Preferred converter configuration is designed for variable solar irradiations at constant temperature.

II. Proposed Radial Basis Function Network Based Hybrid Solar and Battery Operated Dc-Dc Converter System

Standalone PV array systems are of much importance for rural areaswhere it is not Possible or uneconomical to get connect with the Grid Figure 1 shows the block diagram of stand-alone PV power systems, which consists of an array of solar cells, a unidirectional boost converter, a single-phase DC–AC inverter, a storage battery and, most importantly, a bi-directional DC–DC converter. The solar array is connected with the DC bus through the unidirectional DC–DC converter and the battery is also connected with the DC bus through the bidirectional DC–DC converter. Most home appliances operate on AC. Therefore, the DC voltages at the DC bus are converted in AC through the PWM inverter. Stand-alone PV power systems are an important source of electricity for domestic applications—especially in Pakistan, where energy crises are being faced.

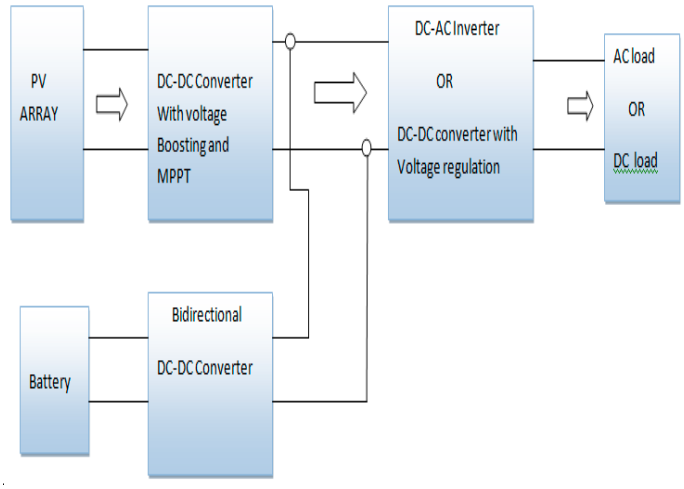

Figure 1. Block Diagram of Proposed System

2.1 Modes of operation

Figure 2 shows the circuit diagram of a proposed two-phase bidirectional DC–DC converter. It is formed by the incorporation of an additional phase from the high efficiency, high-gain converter in [7]. The proposed converter topology is based on the concept of the intermediate storage capacitor and coupled inductor in order to increase its efficiency and output voltage simultaneously. The proposed converter is a two-phase converter, based on a coupled inductor, clamped circuit, output capacitor and an intermediate capacitor for each phase, and it has the additional features of a low magnitude of ripples, with high voltage gain and high efficiency. This bidirectional converter is seen to have a two-phase circuit for the boost mode of operation, while a simple DC–DC converter is used to operate in the buck mode. The battery voltages are stepped up to transfer the power from battery to highvoltage DC link (V_{bus}), whereas the voltages of V_{bus} are stepped down to store the power in the battery.

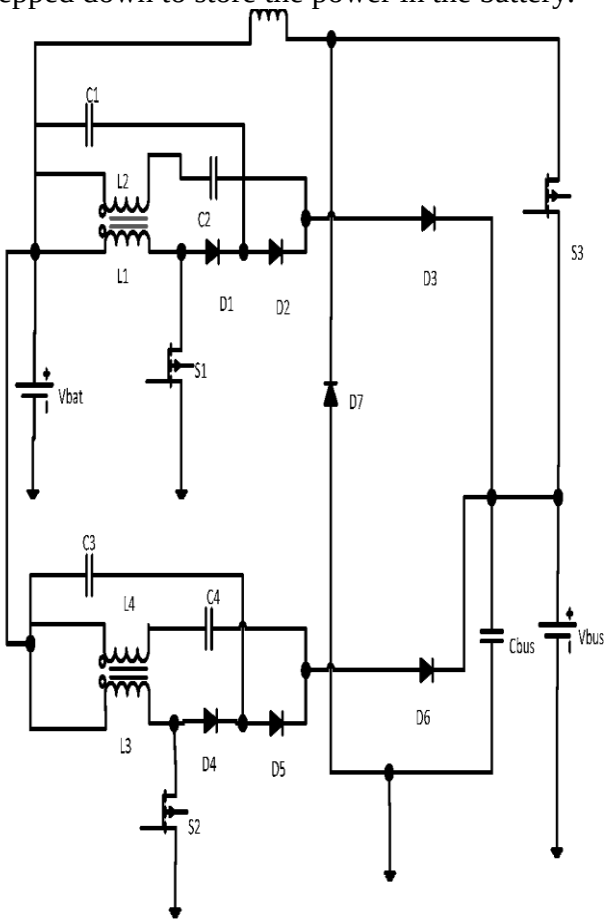

Figure 2 Circuit Diagram of Proposed System

Power switches (s1, s2) will operate the stepped up voltages, while power switch (s3) will operate the stepped down DC-link voltages to high voltage DC link (V_{bus}), whereas the voltages of $V_{bus}$are stepped down to store the power in the battery. Power switches ($s1$, $s2$) will operate the stepped up voltages, while power switch ($s3$) will operate the stepped down DC-link voltages.

2.1.1 Step Down Mode

To step down the voltages from the high voltage DC-link, the power switch (s3), diode D7 and inductor will operate. The circuit diagram for the buck mode of operation is highlighted in Figure 3

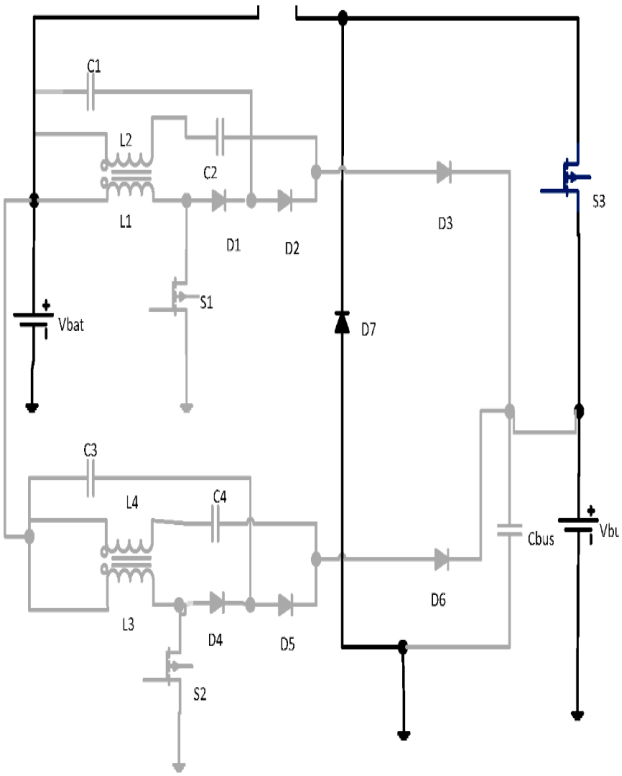

Figure 3. Circuit Diagram of Buck Mode

Mode 1 (Switch closed)

When Switch (s3) is closed, the current I will flow through the inductor L5, while diode D7 will act as an open switch as shown in Figure 4. By applying KVL(Kirchhoff's Voltage Law) to the circuit in Figure 3, Equation (1) is found.

$$V_{1_{L5}} = V_{bus} - V_{bat} \quad \ldots. (1)$$

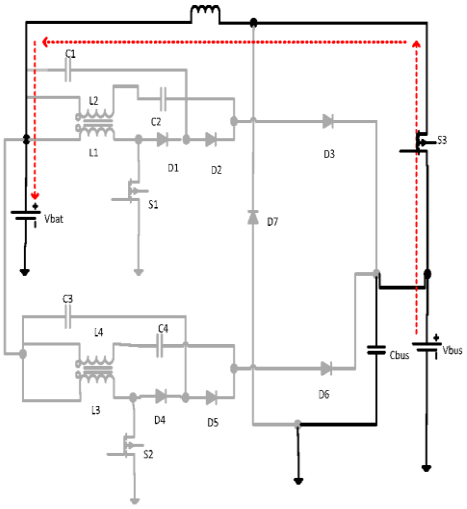

Figure 4. Mode 1 Switch Closed

Mode 2(switch Open)

When switch S3 is opened, the inductor will reverse its polarities and release the stored energy through diode D7, as shown in Figure 5

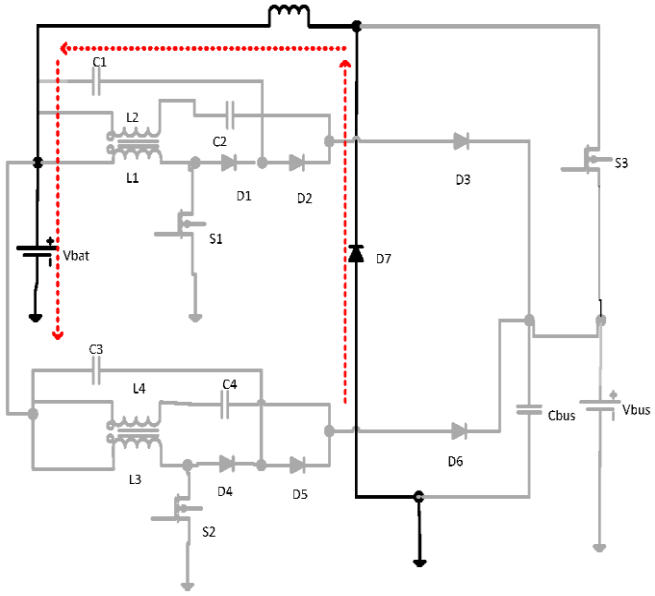

Figure 5 Mode 2 Switch Open

2.1.2 Step Up Mode

We considered the power switches as ideal switches in this analysis. In addition capacitors and inductors as ideal by neglecting the parasitic resistances. Equations of the boost mode of operation at different switching states are presented with the help of circuit diagrams. In this topology, two phases with similar components have been interleaved. Considering the continuous conduction operation of each of the two phases gives five different modes. Each mode has been shown using circuit diagrams. Switching signals for both the switches for the boost mode of operation are shown in Figure 6a,b for a 75 and 50% duty cycle. However, it can be varied. In this analysis, $s1$ is initially off while $s2$ is open, then $s3$.

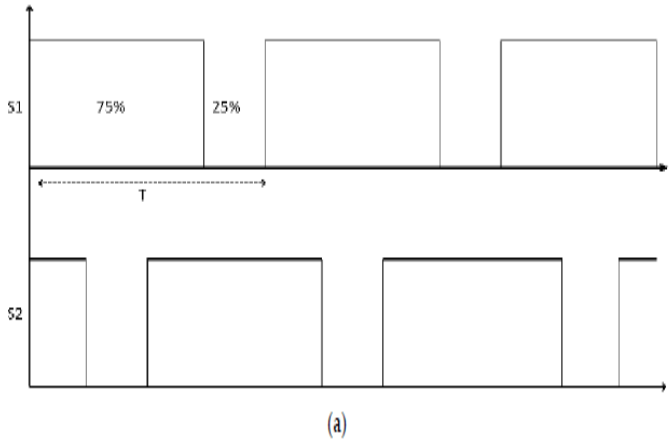

(a)

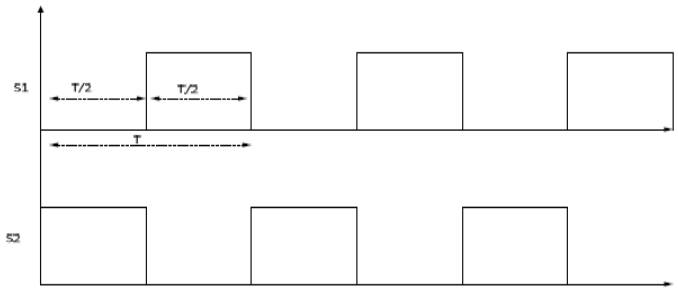
S1
T/2
T/2
T
S2

(b)

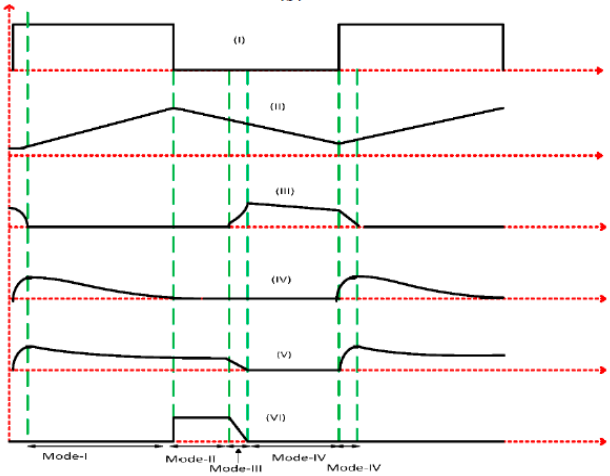
(I)
(II)
(III)
(IV)
(V)
(VI)
Mode-I
Mode-II
Mode-III
Mode-IV
Mode-IV

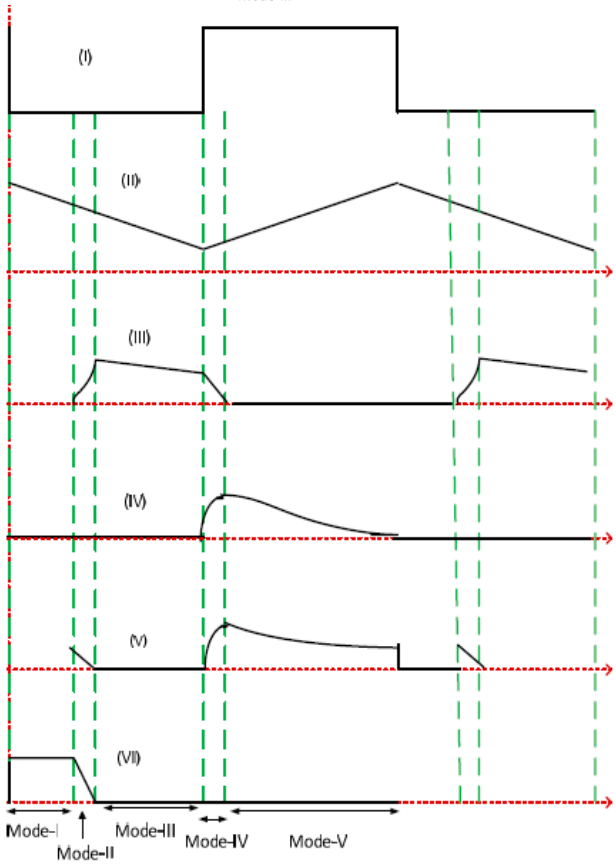
(I)
(II)
(III)
(IV)
(V)
(VII)
Mode-I
Mode-II
Mode-III
Mode-IV
Mode-V

(d)

Figure 6. (**a**) Switching signal for a 75% duty cycle. (**b**) Switching signal for a 50% duty cycle. (**c**)Waveforms for the continuous conduction mode (Phase I): (i) Switching signal; (ii) Magnetizinginductance current; (iii) Current through $D3$; (iv) Current through diode $D2$; (v) Primary inductor L current; (vi) Current through diode $D1$. (**d**) Waveforms for the continuous conduction mode (PhaseII): (i) Switching signal; (ii) Magnetizing inductance current; (iii) Current through $D6$; (iv) Currentthrough diode $D5$; (v) Primary inductor $L3$ current; (vi) Current through diode D4.

2.2 Design Considerations

The proposed converter topology is designed for a load of 300 W keeping in mind the DC bus link is operated in the range of 380–400 V. When the bidirectional converter is operated in the buck mode, it will store the energy in a battery bank. Initial parameters for the proposed DC–DC converter are based on the operation of stand-alone PV power systems–in which, the storage battery bank is operated at different voltages. Commercially available batteries have a rated voltage of 12 V. However, these batteries are connected in series and parallel combinations to operate at different voltage levels. The battery bank operating voltage of nearly every stand-alone PV power systems is around 40 Volts. The coupled inductor design is of the utmost importance. Hence, it can be designed by a flow chart. The proposed converter is implemented and simulated in matalb. Figure 7 shows the boost mode implementation and Figure 8 shows the implementation of the buck mode in ORCAD

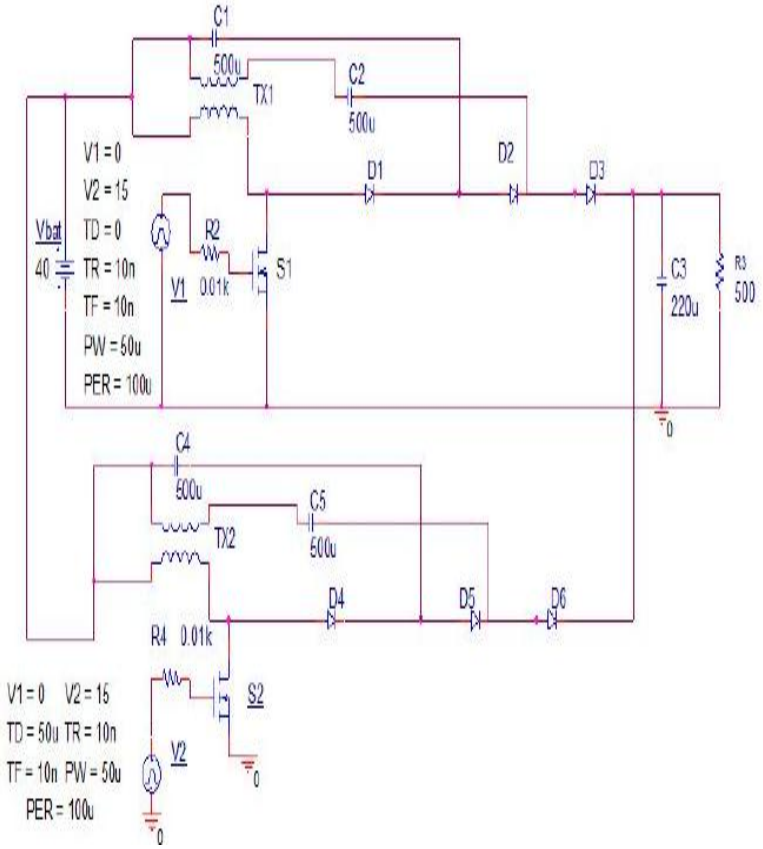

Figure 7 Boost Mode

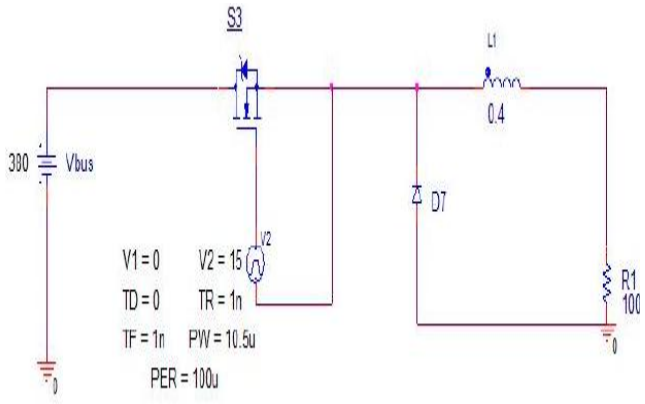

Figure 8. Buck Mode

III. RESULTS AND DISCUSSION

In the previous sections, we analyzed the proposed topology mathematically in terms of voltage gain, magnitude of output voltage ripples, magnitude of output current ripples and component stress. This section describes the verification of the mathematical analysis with its simulated results in mat lab. Finally, the results will be compared with the results of conventional converters. The results of the proposed bidirectional converter will be presented in two stages. In the first stage, the results for the boost mode operation of the converter will be discussed and then the results of the buck mode of operation will be presented and discussed.

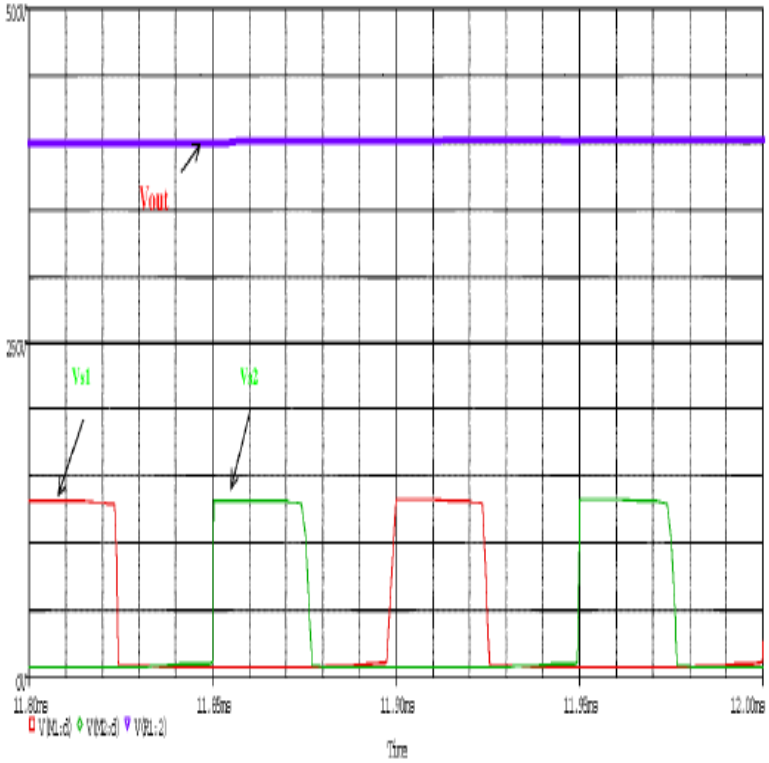

Figure 9 Output voltage waveform across load and voltages across switch

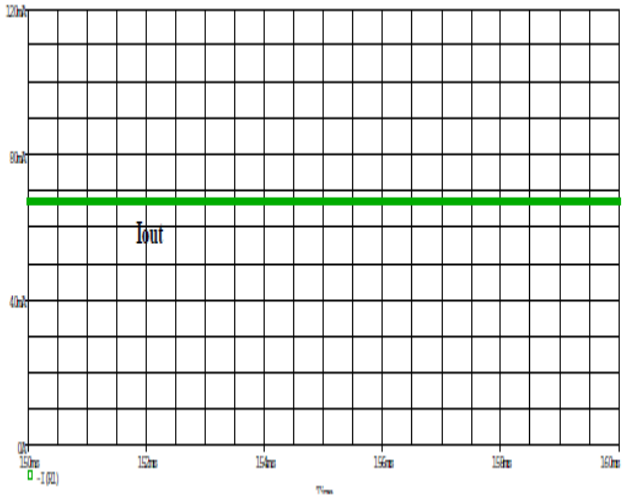

Figure 10a)

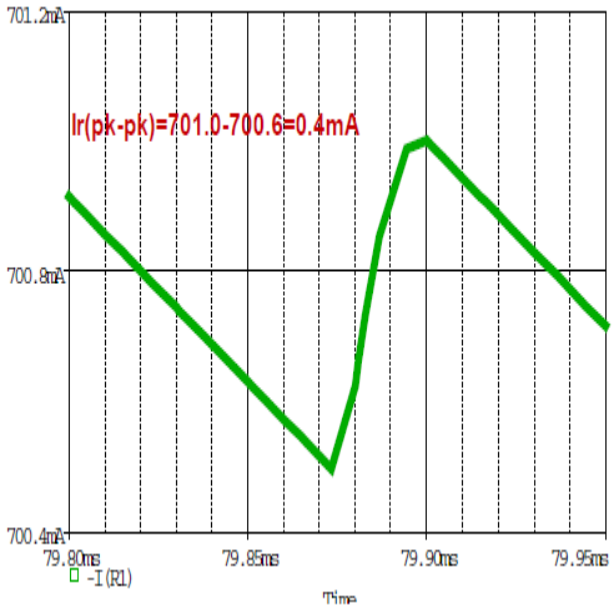

Figure 10b)

Figure 10. (a) Output current waveform. (b) Magnitude of output ripples for proposed converter.

For stand-alone PV power systems, the voltages at the DC bus must be in the range of 380 to 400 V while the input voltage should be in the range of 40 to 50 V. The storage batteries that are commercially available have the voltage ratings of 12 V. However, these voltages are connected in series to provide an input voltage of 40 to 50 V. One of our desired outcomes is that, when the converter with bidirectional power flow is operated in the boost mode, then its voltage gain must be high enough to meet the voltage level of the DC link without exposing the power switches for extreme duty cycles. Figure 9 shows the output voltage of the boost mode of operation by setting the turn ratio of the coupled inductor to four and operating it for a 50% duty cycle. Theoretically, the voltage at the output terminal should be 400 V. Figure 9 is the proof of the mathematical design in which each of the switches are operated for a 50% duty cycle. The output current of the boost mode is shown in Figure 10, in which the voltage across the load is 400 V for a resistive load of 560 W selected by keeping in mind a load of 285 W.

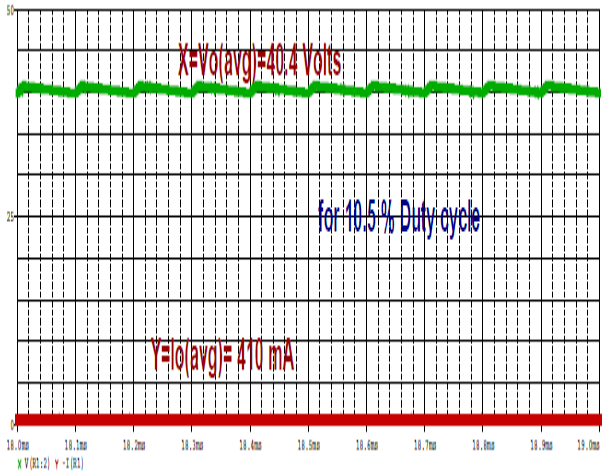

Figure 11. Voltage across battery and current through battery for a 10% duty cycle

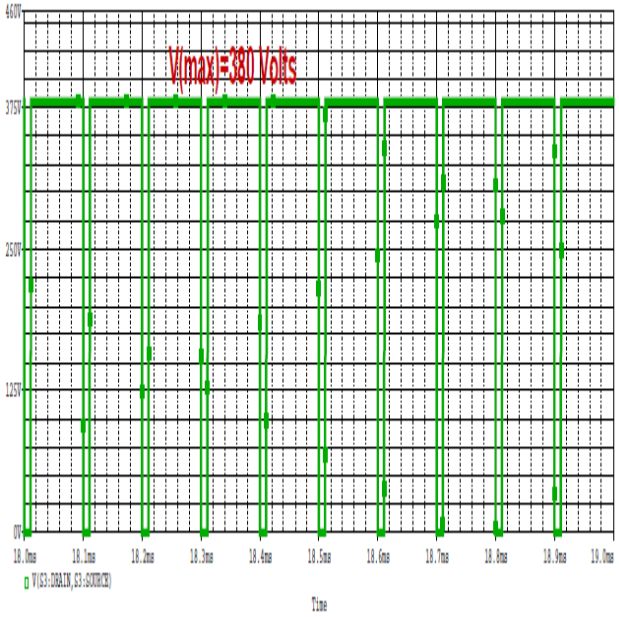

Figure 12. Voltage across *S*3.

The buck mode of operation, the bus voltage of PV power systems, which is around 400 V, is required to be stepped down to store the energy in batteries. Therefore, to step down the voltage of the DC bus from 400 to 40 V it is mandatory to set the minimum duty cycle to 10%. Figure 11 illustrates the output voltage and output current of a bidirectional converter operated in the buck mode. The switch (*S*1) used for the conversion of higher voltage to lower voltage must be rated for over 400 V because when the switch is in the non-conduction state, the high voltage link of the DC bus appears across it. Figure 12 shows the voltage across *S*3, in which 400 V are applied across the switch in the off state, while in the conduction state, it will act as short circuit.

IV. Conclusion

In this research, the main objectives were to explore and propose a novel topology for a bidirectional DC–DC converter with the features of high voltage gain when operated in the boost

mode, without exposing the semiconductor switches to extreme duty cycles, low magnitude output voltage ripples, low stress on the semiconductor switches and increased the power density. With the above objectives in mind, the authors reviewed the available literature of isolated and non-isolated DC–DC converters and concluded that non-isolated DC–DC converters are more appropriate for the application of renewable energy sources and explicitly for stand-alone PV power systems. After reviewing the literature incorporating previous converter designs, a novel interleaved DC–DC converter has been proposed and, by selecting the optimum valued components, the design has been verified in matlab. The authors have achieved their main objectives in which a high voltage gain has been obtained for a duty cycle of 50% or less by changing the turn ration of coupled inductor. The magnitude of current and voltage ripples has been measured and compared with traditional converters and our proposed converter offers a low magnitude of ripples as compared to the present converters. Finally, a reduction in stress on the power switches has been achieved in this research, which is significant to increasing its efficiency.

REFERENCES

[1] Renewable Energy and Other Alternative Energy Sources. In Handbook Alternative Energy; Chapter 12; ABC-CLIO: Santa Barbara, CA, USA, 2008; pp. 149–157.
[2] Anderson, D. Clean Electricity from Photovoltaics; Archer, M.D., Hill, R.D., Eds.; London Imperial College Press: London, UK, 2001.
[3] Markvart, T. Solar Electricity;Willey: New York, NY, USA, 2000.
[4] Zhu, M. Simulation of PV array Characteristics and fabrications of microcontroller based MPPT J. In Proceedings of the 2012 International Conference on Electrical and Computer Engineering, Chengdu, China, 16–28 December 2010.
[5] Zhao, Q.; Lee, F.C. High-e_ciency, high step-up dc-dc converters. IEEE Trans. Power Electron. **2003**, 18, 65–73.
[6] 6. Lee, W.; Han, B.; Cha, H. Battery ripple current reduction in a three-phase interleaved dc-dc converter for 5 kW battery charger. In Proceedings of the 2011 IEEE Energy Conversion Congress and Exposition (ECCE), Phoenix, AZ, USA, 17–22 September 2011; pp. 3535–3540.
[7] Moumita, D. Novel High-Performance Stand-Alone Solar PV System with High-Gain High-Efficiency DC–DC Converter Power Stages. IEEE Trans. Ind. Appl. **2015**, 51, 4718–4728.
[8] J. L. Ny, E. Feron, and E. Frazzoli, "On the Dubins traveling salesman problem," IEEE Trans. Autom. Control, vol. 57, no. 1, pp. 265–270, Jan. 2012.
[9] S. Karaman, M. R. Walter, A. Perez, E. Frazzoli, and S. Teller, "Anytime motion planning using the RRT∗," in Proc. IEEE ICRA, May 2011, pp. 1478–1483.
[10] R. A. Knepper and A. Kelly, "High performance state lattice planning using heuristic look-up tables," in Proc. IEEE/RSJ IROS, 2006, pp. 3375–3380.
[11]. D. Hsu, T. Jiang, J. Reif, and Z. Sun, "The bridge test for sampling narrow passages with probabilistic roadmap planners," in Proc. IEEE ICRA, Sep. 2003, vol. 3, pp. 4420–4426.
[12] L. Zhang, Y. J. Kim, and D. Manocha, "A hybrid approach for complete motion planning," in Proc. IEEE/RSJ IROS, Oct. 2007, pp. 7–14.
[13] S. Dalibard and J.-P. Laumond, "Linear dimensionality reduction in random motion planning," Int. J. Robot. Res., vol. 30, no. 12, pp. 1461–1476, Oct. 2011.
[14] J. Lee, O. Kwon, L. Zhang, and S.-E. Yoon, "A selective retraction-based RRT planner for various environments," IEEE Trans. Robot., vol. 30, no. 4, pp. 1002–1011, Aug. 2014
[15] .L. Mandow and J. P. de la Cruz, "Multicriteria heuristic search," Eur. J. Oper. Res., vol. 150, no. 2, pp. 253–280, Oct. 2003.
[16] S. Yoon and D. H. Shim, "SLPA∗: Shape-aware lifelong planning A∗ for differential wheeled vehicles," IEEE Trans. Intell. Transp. Syst., vol. 16, no. 2, pp. 730–740, Apr. 2015.
[17] R. N. Jazar, Vehicle Dynamics: Theory and Applications. Berlin, Germany: Springer-Verlag, 2008.